



Effect of the combination of geogrid and rubber granules on the performance of ballast under impact loads

Chang Li¹ · Rui Gao¹ · Qihang Hu¹ · Jing Chen²

Received: 23 September 2023 / Accepted: 30 October 2023 / Published online: 18 December 2023
© The Author(s), under exclusive licence to Springer-Verlag GmbH Germany, part of Springer Nature 2023

Abstract

Impact loads can exacerbate the deterioration and deformation of railway ballast, leading to changes in the mechanical properties of the track bed. Geogrid and rubber granules (RG) have been widely used in research to enhance the performance of ballast, however, the effects and mechanisms of these two materials working together are not yet clear. Therefore, in this study, a series of drop hammer impact tests were carried out on ballast aggregates with geogrids and RG. The tests were set up with different geogrid placement locations and RG contents on rigid and flexible subgrades. During the tests, the deformation, impact force and impact time of specimens were measured and recorded, the ballast specimens were sieved after the tests to investigate the breakage of the ballast, and the mechanical properties of the ballast specimens were analyzed after the impact using stiffness and damping ratio. It was found that the deformation and breakage of ballast specimens were significantly reduced by the combination of geogrid and RG, which was better than the geogrid or RG alone, and that the RG improved the damping ratio of ballast, while the geogrid reduced the reduction of stiffness of ballast caused by the addition of RG. Comparing and analyzing the results of each group of tests, the study confirmed that RG with 10% by volume and geogrid placed at 100 mm from the subgrade were the best combination to enhance the ballast performance.

Keywords Ballast · Geogrid · Rubber granules · Impact loads

List of symbols

m	Weight of the hammer	\dot{x}	Velocity of the hammer
b	Damping factor	\ddot{x}	Acceleration of the hammer
k	Stiffness factor	ω_0	Angular frequency of undamped oscillations
t	Time variable	ω	Angular frequency of damped oscillations
t_c	Impact duration	β	Damping coefficient in the Kelvin–Voigt model
v_0	Initial velocity of the hammer	I	Impulse of the hammer
x	Displacement of the hammer	η	Damping ratio

✉ Rui Gao
gaorui@whu.edu.cn; gauryrui@163.com

Chang Li
1690469750@qq.com

Qihang Hu
huqihang@whu.edu.cn; huqihang01@qq.com

Jing Chen
j.chen9412@zju.edu.cn

¹ The Key Laboratory of Safety for Geotechnical and Structural Engineering of Hubei Province, School of Civil Engineering, Wuhan University, Wuhan 430072, China

² Department of Civil Engineering, Zhejiang University, Hangzhou 310058, China

1 Introduction

In recent years, with the increase of train running speed and axle weight, the deterioration of ballast has been accelerated, which seriously affects the safety performance and service life of ballasted track, making track maintenance more frequent and greatly increasing the maintenance cost [1, 2]. Ballast is an important part of ballasted railroads, and its main role is to transfer train loads to the subgrade at a lower stress level, while promoting track drainage and providing a certain degree of lateral resistance [3–5]. Upon repeated train loading of trains, ballast undergoes continuous abrasion and degradation, leading to the fouling of the track, which can cause a significant reduction in the bearing capacity of

the ballast layer and increase the permanent deformation of the track bed. Normally, the magnitude and frequency of the impact loads are higher than the cyclic loads imparted by trains during their normal operation, thus raising the possibility of ballast breakage and resulting in a greater track settlement [6]. The main causes of impact loads are irregularities in wheels or rails (e.g., non-round wheels, rail corrugations, defective rail welds, etc.) and variations in rail stiffness (e.g., transition zones, crossing intersections, bridge and tunnel entrances, etc.) [2, 5, 7]. It should be mentioned that impact loads are unavoidable with a high probability of occurrence. Therefore, it is imperative to carry out a comprehensive study on the performance of ballast aggregates under impact loads and seek practical approach for the associated track issues. Similarly, ballast degradation can be severe in some cases of high subgrade stiffness, such as concrete bridge decks.

In order to reduce ballast degradation and increase track life, it has become common to add geogrids or rubber granules (RG) to the ballast. Earlier studies have shown that geogrids can improve the shear strength of ballast [8–10], increase the modulus of elasticity [11], and reduce deformation and breakage [10–12]. Geogrids also help reduce differential settlement along the length of the track [10]. The mechanism of geogrid is mainly to limit the movement of ballast particles and increase the friction between ballast particles, thus improving track stability [10, 13]. Rubber granules increase the damping ratio and energy dissipation of ballast [14–19], and reduce ballast breakage [15–23]. Rubber granules increase the ballast coordination number and reduce the contact force between ballast particles [21]. However, there are some shortcomings of geogrid or rubber granules in enhancing the performance of ballast. Nimbalkar et al. [24, 25] found limited reduction of ballast breakage by geogrids on rigid subgrade through field tests. Ngo et al. [5] and Indraratna et al. [2] found through indoor impact tests that the peak impact force did not change significantly with and without geogrids, thus showing the limited ability of geogrids to absorb impact stresses. And rubber granules reduce the shear strength and friction angle of ballast and increase its settlement and deformation, mainly because the modulus of elasticity of rubber granules is lower than that of ballast particles [14, 21, 22].

From previous studies, it can be concluded that geogrid and rubber granules can compensate for each other's deficiencies. Rubber granules reduce the shear strength of the ballast and increase the deformation of the ballast, while geogrid increases the shear strength of the ballast and reduces the deformation of the ballast; Geogrid has a limited ability to absorb impact forces, while rubber granules can increase ballast damping ratio and energy dissipation. However, there is a lack of research on how the combination of geogrid and rubber granules affects the performance of

ballast. Therefore, in this study, geogrid and rubber granules were added together into the ballast to investigate the effects of the combination of geogrid and rubber granules on the deformation, breakage, stiffness and damping ratio of the ballast under impact loads by using a drop hammer impact test setup. Different geogrid positions and rubber granules contents were set up to find the optimum combination of materials to improve the ballast performance.

2 Materials and testing program

2.1 Test materials

The main materials used in this test were fresh ballast, rubber granules and geogrid. The ballast (Fig. 2a–b) was taken from a quarry in Wuhan, Hubei Province, China, and is made of granite. The specific gravity of ballast was measured as 2.66, and the compaction density was 1600 kg/m^3 . The compacted density was taken from the average density obtained from five operations of filling ballast into the mold to reduce the operation error and reflect the true density of the specimen. The ballast gradation is in accordance with China Railway Ballast Standard (TB/T 2140-2008), and the measured ballast gradation is shown in Fig. 1. The maximum particle size of ballast D_{\max} is 63 mm, the minimum particle size of ballast D_{\min} is 16 mm, and the average particle size of ballast D_{50} is 40 mm. the ballast is cleaned and dried before the test.

Rubber granules (Fig. 2d) are obtained by cutting waste recycled tires and have a specific gravity of 1.15. Kho-shoei et al. [26] found that rubber granules of larger size (20–60 mm) were not as hard as rubber granules of smaller size (10–20 mm). Sánchez et al. [27] found that rubber granules with a particle size above 8 mm did not contaminate the ballast. Considering that the minimum size of the ballast is 16 mm, the range of the rubber granules' particle sizes in this test was 8 mm–16 mm. Gong et al. [21] and Koohmishi et al. [20] suggested 10% by volume of rubber granules as the optimum content, Arachchige et al. [22] considered 10% by weight as the optimum content while Song et al. [14] suggested 5% by volume as the optimum content. The above studies have focused on the interaction between rubber granules and ballast, without considering the addition of geogrid, so in order to explore the effect of different rubber granule content on the effect of the combination of geogrid and rubber granules, the rubber granules are taken as a percentage of the volume of the four cases of 0%, 5%, 10%, and 15% in the current test.

The geogrid (Fig. 2c) is a polypropylene biaxial geogrid with specific mechanical parameters shown in Table 1. Some studies [28–30] have shown that the optimum aperture of geogrid for ballast reinforcement is $1.4D_{50}$, so a

Fig. 1 Particle size distribution of ballast

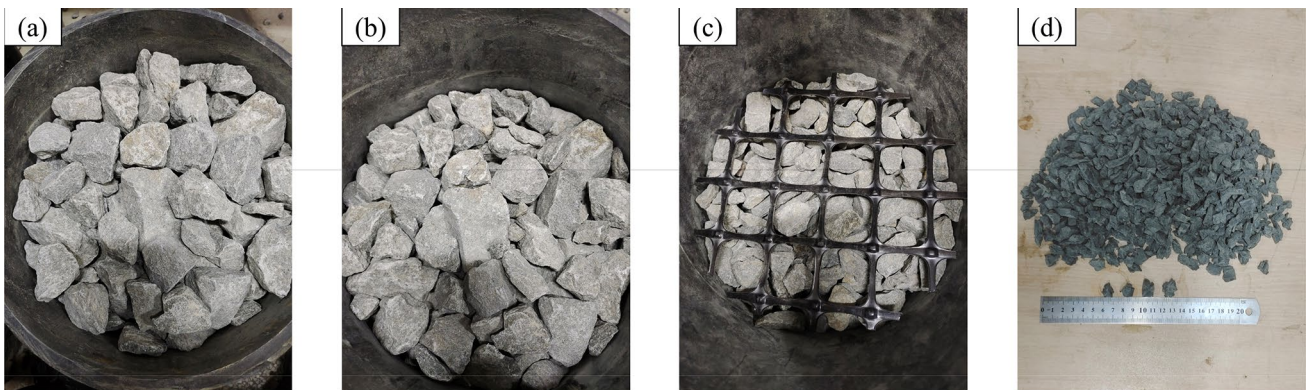
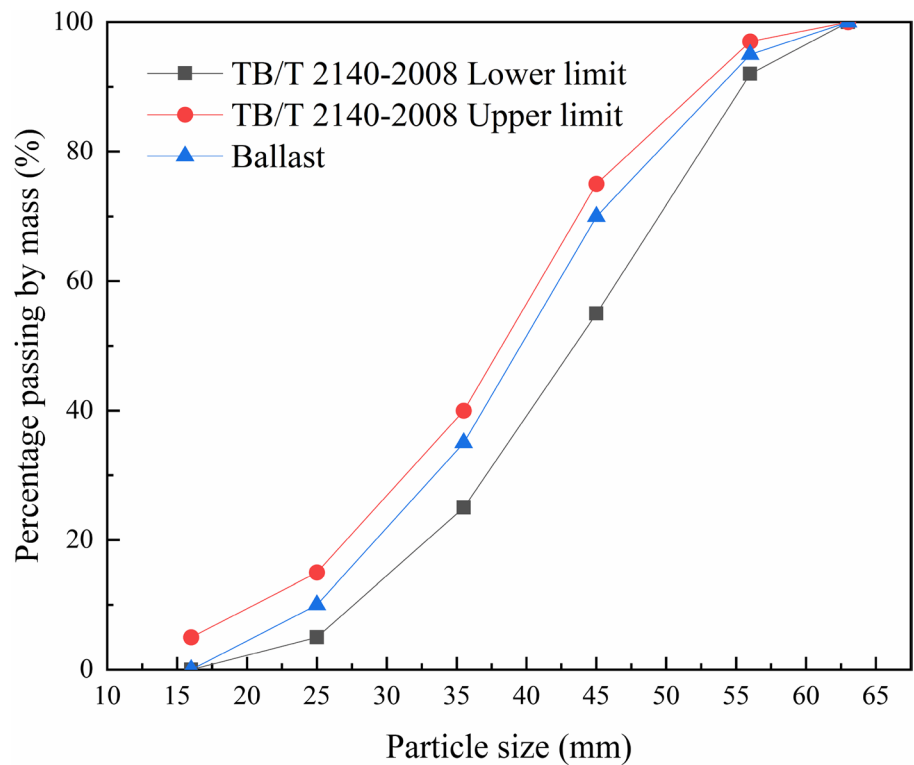


Fig. 2 Test materials: **a** ballast before impact; **b** ballast after impact; **c** geogrid; **d** rubber granules

Table 1 Physical and mechanical properties of geogrids

Property	Value
Structure	Biaxial geogrid
Geogrid aperture size	55 mm × 55 mm
Material	Polypropylene
Tensile strength at 2% strain	11 KN/m
Tensile strength at 5% strain	15 KN/m
Peak tensile strength	30 KN/m
Strain at peak	13%

geogrid with an aperture of 55 mm was used in this test. Ngo et al. [5] and McDowell et al. [31] found that the optimum placement of geogrids is 100 mm above the subgrade and Chen et al. [28] suggested that the optimum placement of geogrids is 50 mm above the subgrade. In order to investigate the influence of different laying positions of geogrid on the combined effect of geogrid and rubber granules, the laying positions of geogrid in this test were 50 mm and 100 mm from the subgrade.

2.2 Drop weight impact test apparatus

The drop weight impact test apparatus has a hammer with a mass of 60 kg that can be dropped freely from a maximum height of 2.5 m (Fig. 3a). In order to simulate the lateral confinement conditions in the field and the lateral deformation of the ballast, an 8 mm thick cylindrical rubber mold with a diameter of 300 mm was used for the test. A circular steel plate is placed at the upper end of the specimen to transfer the impact loads more uniformly to the ballast specimen, and a dynamic force sensor is installed on the plate to measure the impact stress generated by the falling weight. The range of this sensor is 250 KN, and Fig. 3b shows the sensor and acquisition system.

2.3 Testing program and procedure

The rubber membrane is fixed to the base, and since the stiffness of the subgrade affects the performance of the ballast improved by the geogrid and rubber granules, Koohmishi et al. [16] has suggested placing a 50 mm thick compacted gravel at the bottom to simulate the sub-ballast layer. Therefore, in this study, 50 mm thick compacted gravel is used as the sub-ballast layer (Fig. 3c), and ballast specimens are placed directly on the base to simulate rigid subgrade, such as concrete bridge decks (Fig. 3d). The mixture of ballast and rubber granules was loaded into the mold in three layers, each layer being 100 mm thick, and compacted with a handheld compactor. It is important to prevent ballast particles from separating from rubber granules during the specimen making process to ensure the homogeneity of the specimen, and in order to prevent the ballast from breaking during compaction, a layer of rubber mat is attached to the compactor. At the end of the last layer of tamping, the loading plate was placed on the specimen and the rubber membrane was fixed with steel hoop. The entire specimen preparation was completed with specimen dimensions of 400 mm in height

and 300 mm in diameter. The impact testing machine and specimen arrangement is shown in Fig. 4.

The initial height of the specimen was measured at four evenly spaced points around the specimen and the circumference of the specimen was measured at three different locations from the top, center and bottom, and these initial measurements were recorded for reference. Raising the hammer to a height of 900 mm and then dropping it freely can generate a stress of approximately 550 kPa to simulate typical impact stresses due to wheel-rail defects or stiffness changes [32]. The specimen was subjected to 20 impacts per test, as the specimen no longer deformed significantly after more than 20 impacts. The height and circumference of the specimen were measured and recorded after each impact and compared with the initial values to determine the axial and radial deformation of the ballast specimen during impact. The ballast was collected after the test was completed, then it was carefully sieved and weighed. The sub-ballast in our tests were compacted gravels, which normally had smaller particle sizes than the broken pieces of ballast. In addition, the sub-ballast gravel and the ballast materials were sprayed with different colors during our tests, with the gravel being yellow and the ballast being gray. After the impact tests, we manually picked out the broken pieces of ballast after sieving the mixture of gravel and the broken pieces of ballast. A total of 16 tests were conducted to investigate the effect of geogrids and rubber granules on ballast performance under impact loading. The specific test groupings are shown in Table 2.

2.4 Methods for evaluating stiffness and damping ratio of ballast specimens

Stiffness reflects the stability of the roadbed, which is essential for railroad safety and also affects the comfort of train operation. Damping ratio can be used to evaluate the energy dissipation efficiency of ballast specimens in dynamic analysis. The

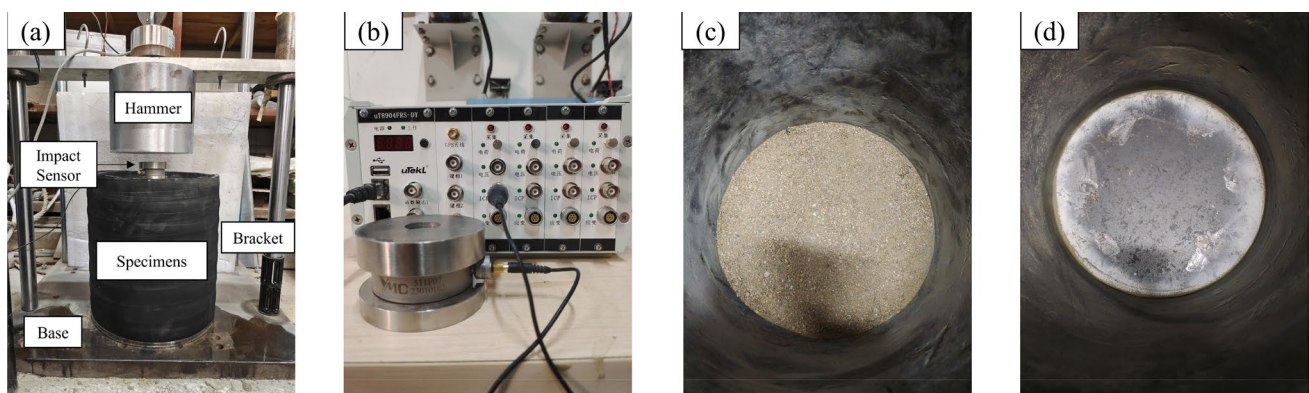


Fig. 3 Test equipment and materials: **a** test apparatus; **b** sensor and acquisition system; **c** flexible subgrade; **d** rigid subgrade

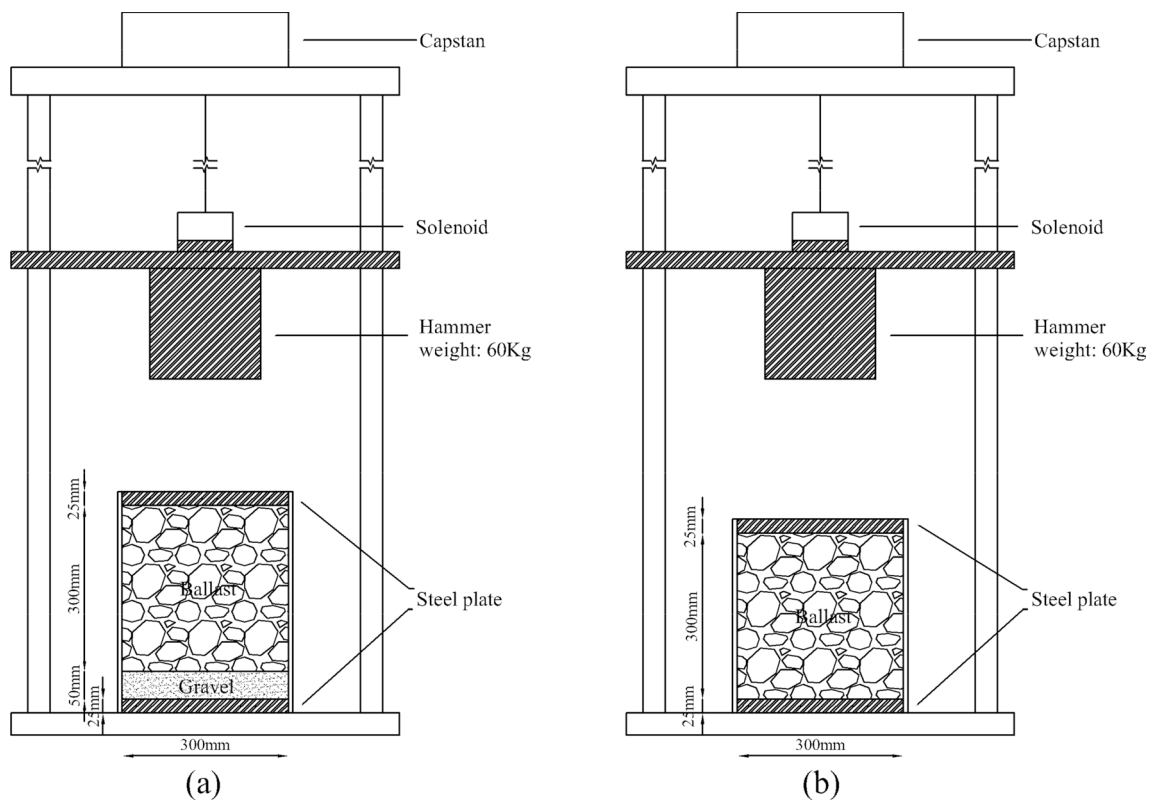


Fig. 4 Schematic diagram of impact testing machine and specimen layout: **a** flexible subgrade; **b** rigid subgrade

Table 2 Test plan and test configurations

Test number	Subgrade type	Geogrid position	Rubber granule content (%)
T1	With sub-ballast	Without geogrid	0
T2	With sub-ballast	Without geogrid	5
T3	With sub-ballast	Without geogrid	10
T4	With sub-ballast	Without geogrid	15
T5	With sub-ballast	50 mm above the subgrade	0
T6	With sub-ballast	50 mm above the subgrade	5
T7	With sub-ballast	50 mm above the subgrade	10
T8	With sub-ballast	50 mm above the subgrade	15
T9	With sub-ballast	100 mm above the subgrade	0
T10	With sub-ballast	100 mm above the subgrade	5
T11	With sub-ballast	100 mm above the subgrade	10
T12	With sub-ballast	100 mm above the subgrade	15
T13	Without sub-ballast	Without geogrid	0
T14	Without sub-ballast	Without geogrid	10
T15	Without sub-ballast	100 mm above the subgrade	0
T16	Without sub-ballast	100 mm above the subgrade	10

damping performance of the roadbed affects track vibration, and an appropriate damping ratio can attenuate the impact loads during train operation and reduce the deterioration of the

roadbed [33]. In order to evaluate the change in stiffness and damping ratio of ballast specimens after the addition of rubber granules and geogrids, the specimens were simplified to a

viscoelastic impact model. Koohmishi et al. [16] and Argatov et al. [34] have simplified the specimen to Maxwell and Kelvin viscoelastic models. Most studies have used the Kelvin model [35, 36], which will also be used in this study, and the model is shown in Fig. 5.

The differential equation for the collision according to Newton's second law is as follows [34]:

$$m\ddot{x} + b\dot{x} + kx = 0, t \in [0, t_c] \tag{1}$$

where m is the hammer mass, b is the damping factor, k is the stiffness factor, and t_c is the impact duration. The initial conditions for Eq. (1) are as follows:

$$x(0) = 0, \dot{x}(0) = v_0 \tag{2}$$

$$\ddot{x}(t_c) = 0 \tag{3}$$

Solutions to Eqs. (1) and (2):

$$x(t) = \frac{v_0}{\omega} \exp(-\beta t) \sin \omega t, t \in [0, t_c] \tag{4}$$

$$\omega_0^2 = \frac{k}{m}, \omega^2 = \omega_0^2 - \beta^2, \beta = \frac{b}{2m} \tag{5}$$

Through the differential Eq. (4):

$$\dot{x}(t) = \frac{v_0}{\omega} \exp(-\beta t)(\omega \cos \omega t - \beta \sin \omega t) \tag{6}$$

Through the differential Eq. (6):

$$\ddot{x}(t) = -\frac{v_0}{\omega} \exp(-\beta t)[(\omega^2 - \beta^2) \sin \omega t + 2\beta\omega \cos \omega t] \tag{7}$$

Solve Eqs. (3) and (7):

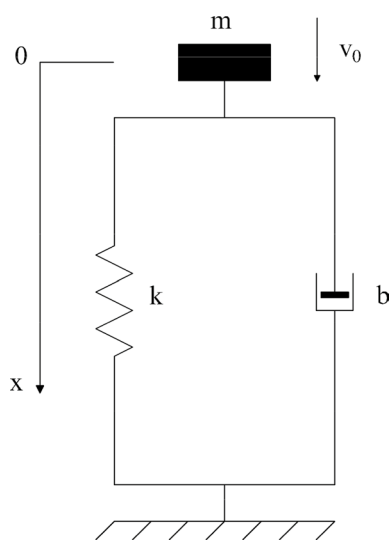


Fig. 5 Schematic diagram of the Kelvin model

$$t_c = \frac{2}{\omega} a \tan \frac{\omega}{\beta} \tag{8}$$

Bringing Eq. (8) into Eq. (6) yields:

$$\dot{x}(t_c) = -v_0 \exp(-\beta t_c) \tag{9}$$

The change in momentum of the hammer throughout the impact is:

$$I = -mv_0[1 + \exp(-\beta t_c)] \tag{10}$$

ω and β can be obtained by bringing the impact duration and the change in hammer momentum measured in the test into Eqs. (8) and (10). bring ω and β into the equations:

$$k = m(\omega^2 + \beta^2), \eta = \frac{b}{2\sqrt{km}} \tag{11}$$

The specimen stiffness k and damping ratio η can be obtained.

After the impact was completed, the hammer drop height was adjusted to 100 mm and the maximum impact force and impact duration of the specimen were measured by a single impact to calculate the stiffness and damping ratio. Considering that the impact force and the number of impacts were much smaller than the formal impact test, the effect on the overall variation of the specimen was negligible.

3 Results and discussion

3.1 Axial and radial deformation

The axial deformation is the difference between the initial height of the specimen and its height after each impact. The radial deformation is the difference between the maximum circumference of the specimen and its circumference before loading. Figure 6 shows the variation of axial and radial deformation of the specimen with the number of falling hammer impacts for different rubber granules contents, from which it can be seen that the deformation of the specimen increases with the increase in the number of impacts. With the rearrangement and compaction of ballast particles, the deformation of the specimen is large at the initial stage, and the deformation rate of the specimen gradually decreases after the number of impacts reaches 10. The maximum reduction in specimen deformation was achieved at a rubber granule content of 10%, with a reduction of 6.38% in axial deformation and 2.31% in radial deformation. It is similar to the study by Koohmishi [20]. This shows that rubber granules do not have a significant effect on reducing the deformation of ballast specimens, although the rubber granules can fill the gap between the ballast, absorb part of the impact energy and reduce the breakage of ballast

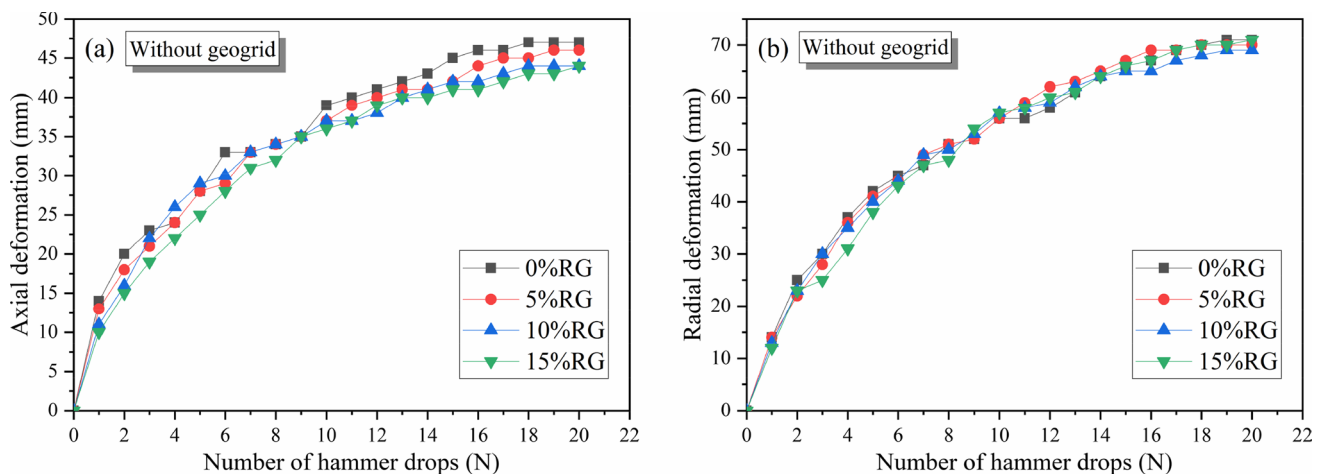


Fig. 6 Deformation of ballast with rubber particles: **a** axial deformation; **b** radial deformation

particles (the effect of rubber granules on ballast breakage is detailed in section 'Ballast breakage'), they reduce the friction between the ballast, so that the overall deformation is not well suppressed.

Figure 7 shows the variation of axial and radial deformation of the specimen with the number of drop hammer impacts with geogrid and rubber granules. When the geogrid was 50 mm away from the subgrade, the 10% rubber granules content had the best suppression of deformation, reducing axial deformation by 19.05% and radial deformation by 17.74% compared to the specimen without rubber granules; When the geogrid was 100 mm away from the subgrade, the 10% rubber granule content also had the best suppression of deformation, reducing axial deformation by 21.95% and radial deformation by 19.67% compared to the specimen without rubber granules. This means that the combination of geogrid and rubber granules has a good inhibiting effect on specimen deformation. It is mainly because geogrid can form interlocking effect with ballast particles, increase the friction between ballast particles, limit the lateral movement of ballast particles, make up for the reduction of friction between ballast particles caused by rubber granules, so that the advantages of rubber granules can be fully utilized. When the content of rubber granules reaches 15%, the deformation of the specimen increases compared to 10% rubber granules, because excessive rubber granules not only reduce the friction between ballast particles, but also weaken the interlocking between the geogrid and ballast particles. Compared with the geogrid at 50 mm from the subgrade, the axial deformation is reduced by 5.88% and the radial deformation is reduced by 3.92% when the geogrid is 100 mm from the subgrade, which can be concluded that the geogrid is more effective in reducing the deformation when it is 100 mm from the subgrade. From Fig. 8, it can be seen that the maximum radial deformation of the ballast specimen

occurs in the lower half of the specimen, and the influence range of the geogrid located at 50 mm is closer to the bottom of the specimen, and the deformation is easy to be generated above the geogrid. Geogrid located at 100 mm reduces the upward shift of radial deformation, which makes the overall deformation more uniform and has a better effect on the reduction of specimen deformation. A similar observation was also reported by Indraratna [12] and Sweta [11]. Therefore, the optimum combination of materials to reduce the deformation of the specimen was 10% by volume of rubber granules and a geogrid 100 mm above the subgrade.

Figure 9 shows the effect of geogrid and rubber granules on the deformation of ballast specimens at different subgrade stiffness. In both rigid and flexible subgrades, the combination of geogrid and rubber granules is more effective in suppressing specimen deformation than geogrid or rubber granules alone. Because geogrid can limit the movement of ballast particles, increase the friction between ballast particles, to make up for the rubber particles on the ballast friction reduction, while the rubber granules to absorb the impact energy is better than the geogrid, and rubber granules can reduce the breakage of ballast particles (the effect of rubber granules on ballast breakage is detailed in section 'Ballast breakage'), the two form a complementary advantage, so as to get better results. From the figure, it can be seen that the deformation of the specimen without sub-ballast is larger than that of the specimen with sub-ballast as a whole, because the sub-ballast can absorb the impact energy and reduce the impact stress, thus reducing the deformation of the specimen. This is in agreement with previous study on sun-ballast [2]. In the case with sub-ballast, the axial and radial deformations of the specimen with geogrid and rubber granules together were reduced by 31.91% and 30.98% compared to the pure ballast specimen; In the case without sub-ballast, the axial and radial deformations of the

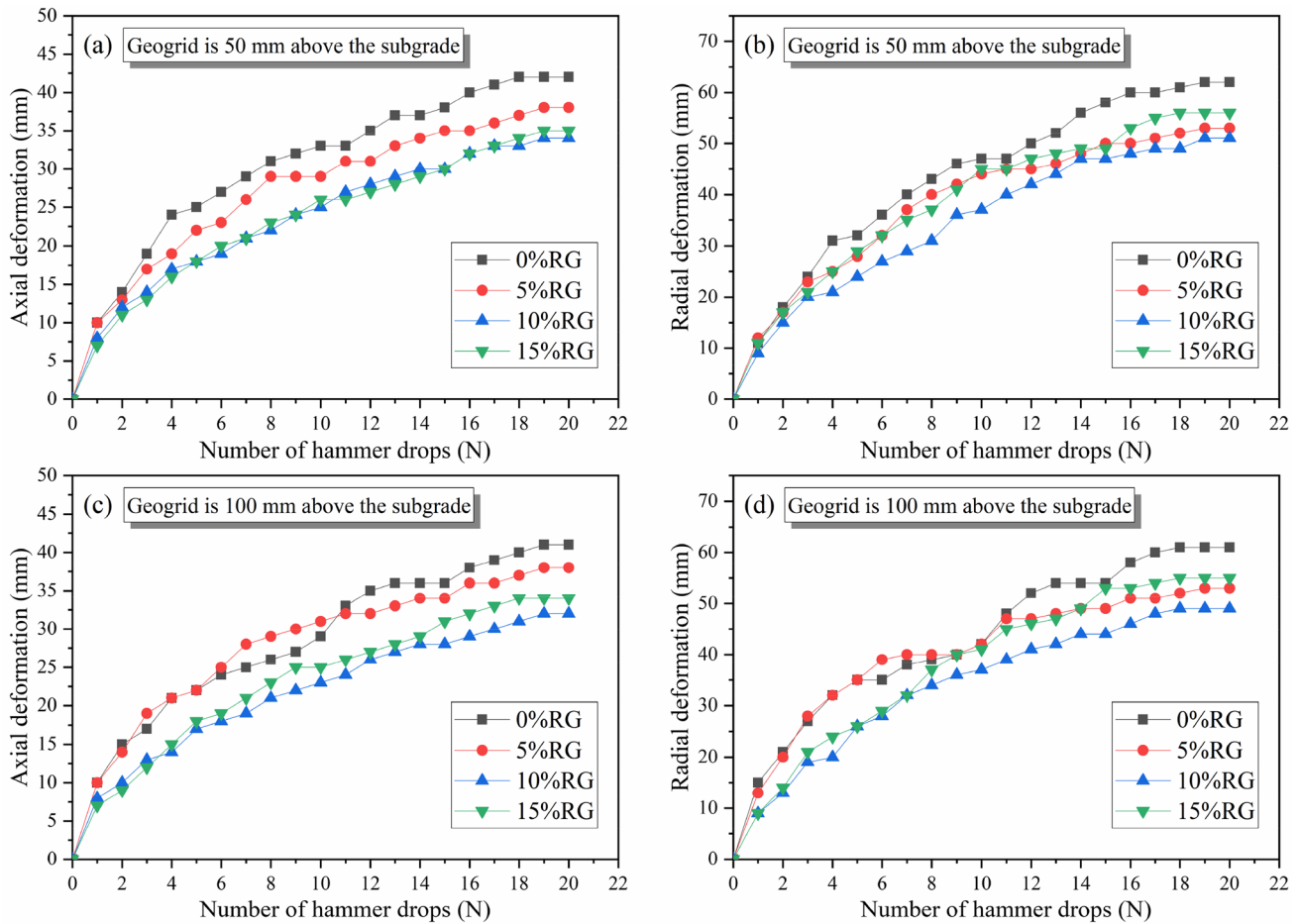


Fig. 7 Deformation of ballast with geogrid and rubber granules: **a, b** Axial and Radial deformation of ballast with geogrid 50 mm from the subgrade; **c, d** Axial and Radial deformation of ballast with geogrid 100 mm from the subgrade

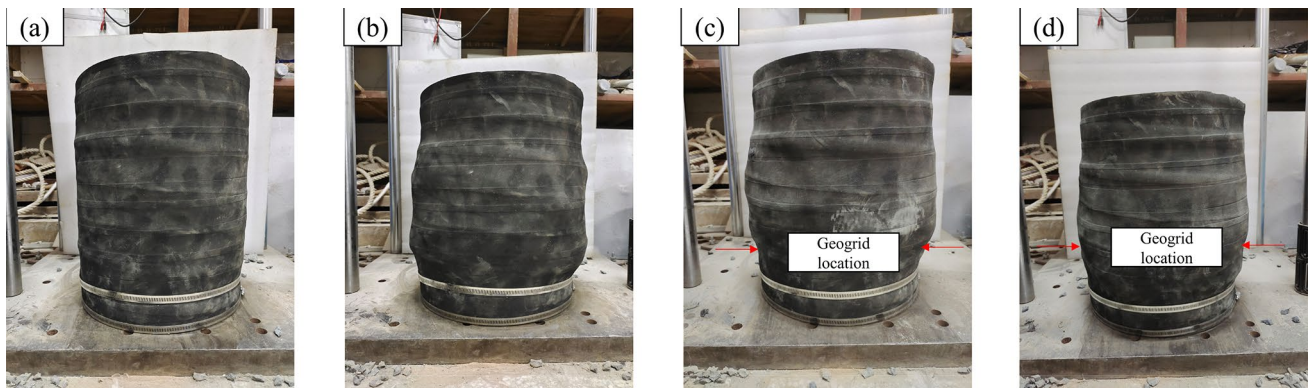


Fig. 8 Deformation of specimens in different test groups: **a** Specimen before impact; **b** 0%RG/without geogrid; **c** 10%RG/with geogrid at 50mm; **d** 10%RG/with geogrid at 100mm

specimen with geogrid and rubber granules together were reduced by 35% and 35.63% compared to the pure ballast specimen. It can be concluded that geogrids and rubber granules are more effective in reducing ballast deformation

on rigid subgrade, because the role of geogrids and rubber granules in absorbing impact energy and reducing impact stress is similar to that of sub-ballast, which makes the role of both of them is not fully utilized.

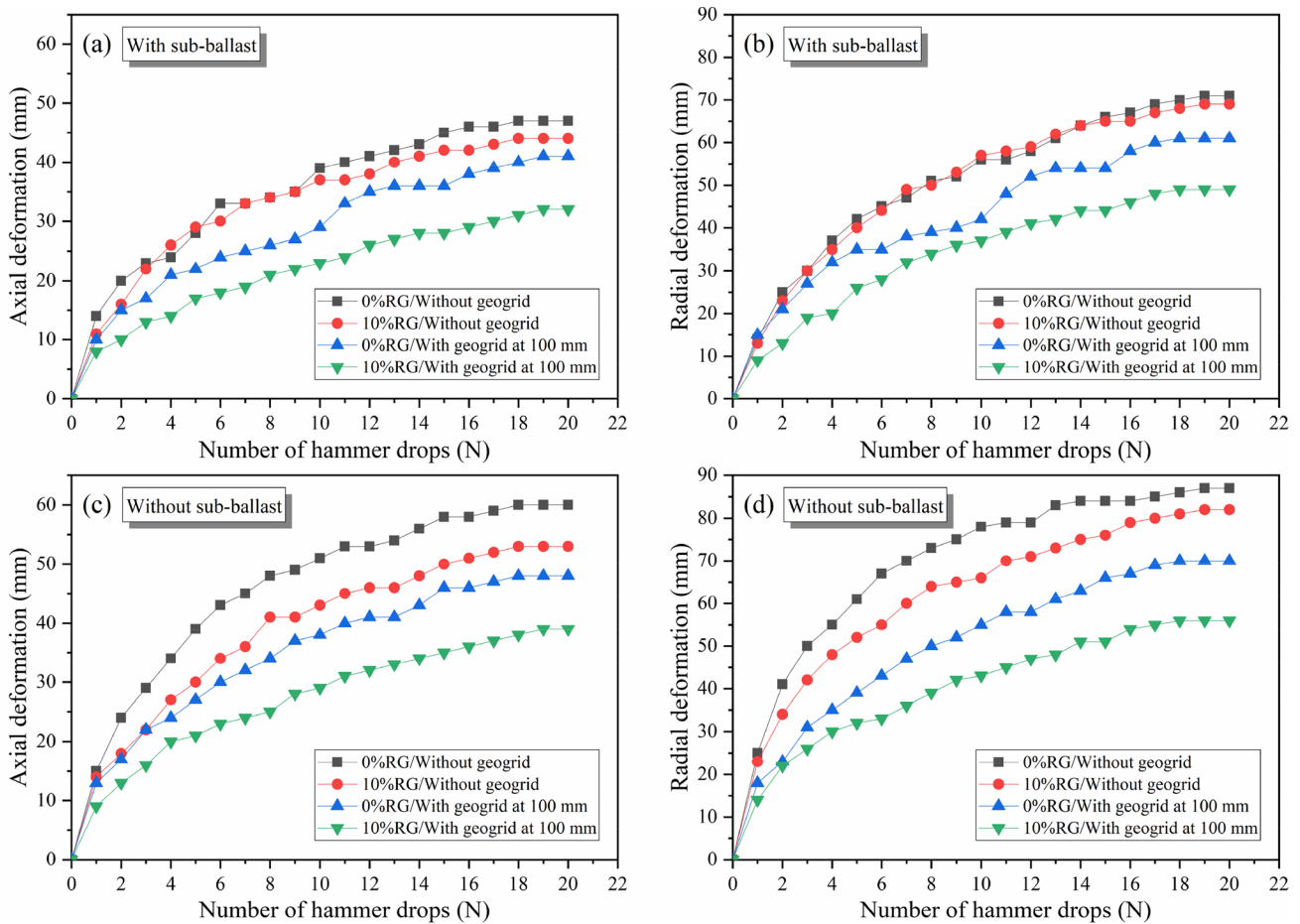


Fig. 9 Deformation of ballast with rubber granules and geogrid on different subgrade stiffness: **a, b** Axial and radial deformation of ballast with sub-ballast; **c, d** Axial and radial deformation of ballast without sub-ballast

3.2 Ballast breakage

In this paper, the ballast breakage index (*BBI*) proposed by Indraratna et al. [37] is used to quantify the degree of ballast breakage. Since *BBI* is suitable for a narrow range of particle sizes and small uniformity coefficients (the ballast in this test has a particle size range of 16–63 mm and a corresponding uniformity coefficient of 1.75) and can better characterize the overall ballast breakage, *BBI* has been used in this paper for the overall ballast breakage analysis of ballast specimens. As shown in Fig. 10, it is obtained by calculating the area enclosed by the grain size distribution curve and the crushed boundary before and after the test:

$$BBI = \frac{A}{A + B} \tag{12}$$

A, the area between the particle size distribution curve before and after the test; B, the area between the particle size distribution curve and the breakage boundary after the test.

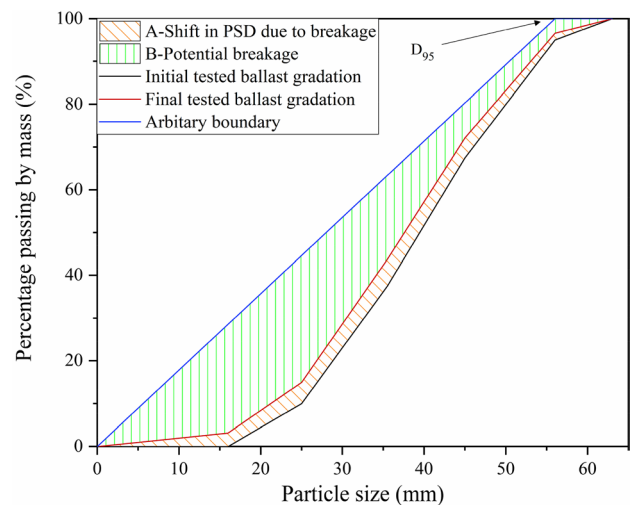


Fig. 10 Quantification of ballast breakage using the ballast breakage index, *BBI*

Figure 11 shows the effect of geogrid and rubber granules on ballast breakage for different subgrade stiffness. From Fig. 11a, it can be seen that the breakage of ballast decreases with the increase of rubber granules content, and the breakage of the specimen with 15% rubber granules content is 52.49% less than that of pure ballast. This trend is similar to that reported by Zhang [23] and Koozmishi [20]. Rubber granules can fill the gap between ballast particles, increase the contact area between ballast, increase the stress distribution, absorb part of the impact energy, thus reducing the breakage of ballast specimens. Without rubber granules, the geogrid reduced ballast breakage by a maximum of 10.19% because the geogrid and the ballast particles can form an interlock, limiting the displacement of the ballast particles and reducing the abrasion of the ballast particle. This is consistent with the finding of Indraratna [2]. Compared with the specimen without geogrid, the ability of geogrid to reduce ballast breakage decreases gradually as the content of rubber granules increases, and when the content of rubber granules reaches 15%, the maximum reduction of geogrid to ballast breakage is 7.44%, which is due to the fact that the increase of rubber granules weakens the interlocking between geogrid and ballast and increases the movement of ballast particles. From Fig. 11b, it can be seen that the breakage of the specimen with sub-ballast is smaller than that of the specimen without sub-ballast. The breakage of the ballast specimen with geogrid and rubber granules together is less than that of the specimen with geogrid or rubber granules alone under the same conditions. Compared with the ballast-only specimens, the reduction in breakage of the specimens with sub-ballast by the combination of geogrid and rubber granules is smaller than that of the specimens without sub-ballast, indicating that the combination of

geogrid and rubber granules is more effective in suppressing ballast breakage on rigid subgrade.

3.3 Stiffness and damping ratio

Figure 12 shows the effect of geogrid placement location and rubber granule content on the stiffness of ballast specimens. From Fig. 12a, it can be seen that the stiffness of ballast specimen decreases with the increase of rubber granules content, and the stiffness of ballast specimen decreases by 19.37%, 37.58%, and 47.60% when the content of rubber granules is 5%, 10%, and 15%, which is due to the fact that the modulus of elasticity of rubber granules is much lower than that of ballast particles. A similar result was reported by Arachchige [15]. The rate of reduction of ballast specimen stiffness decreases when the rubber particle content exceeds 10%. Compared to the ballast specimens without geogrid, the ballast specimens with geogrid 100 mm away from the subgrade showed an increase in stiffness of 18.11%, 14.14%, 11.00%, and 5.42% at 0%, 5%, 10%, and 15% rubber granules content. The degree of improvement of ballast specimen stiffness by geogrid showed a decreasing trend with the increase of rubber granules content. This is due to the fact that the geogrid restricts the movement of the ballast particles and increases the contact stresses between the particles, which enhances the stiffness of the ballast specimen, and as the content of the rubber granules increases, the interlocking between the geogrid and the ballast is weakened, resulting in a lower degree of increase in stiffness. Figure 12b shows the stiffness of ballast specimens with different subgrade stiffness. The stiffness of the specimen without sub-ballast is greater than that of the specimen with sub-ballast because the sub-ballast can absorb the impact energy. The stiffness of the specimens with and without sub-ballast decreased by

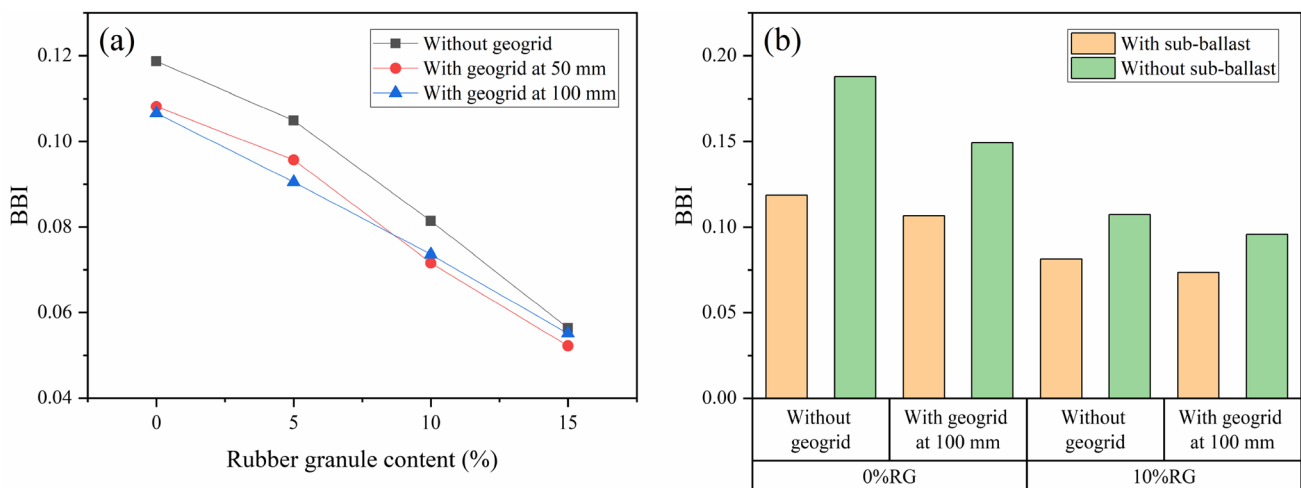


Fig. 11 Breakage of ballast with geogrid and rubber granules: **a** Breakage of ballast with sub-ballast; **b** Breakage of ballast with and without sub-ballast

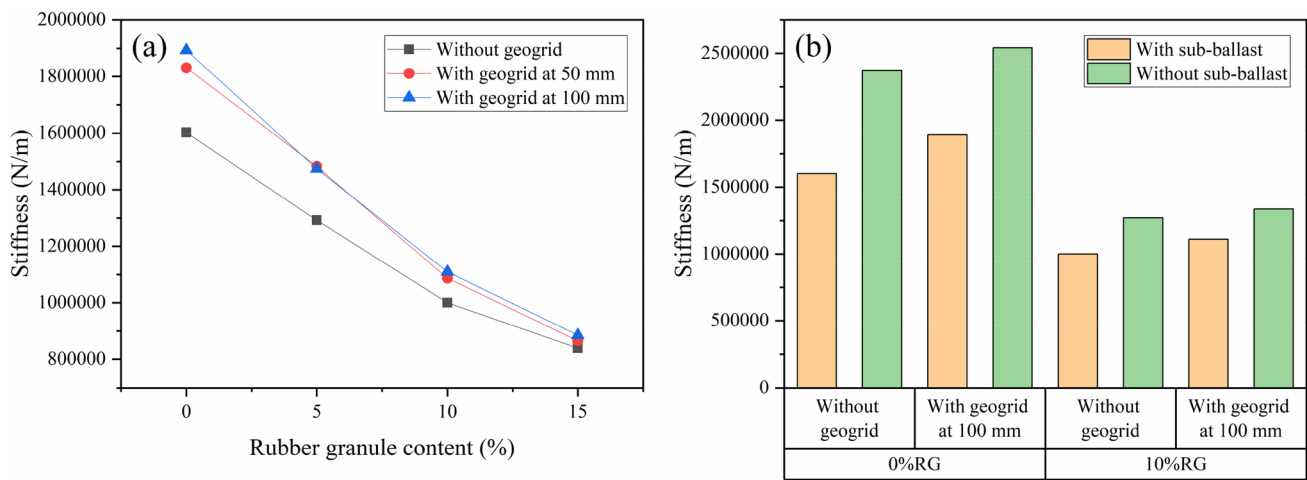


Fig. 12 Stiffness of ballast with geogrid and rubber granules: **a** Stiffness of ballast with sub-ballast; **b** Stiffness of ballast with and without sub-ballast

37.58% and 46.38% with the addition of 10% rubber granules, so the rubber granules have a greater effect on the stiffness of the specimens on a rigid subgrade.

Figure 13 shows the effect of geogrid position and rubber granule content on the damping ratio of ballast specimens. From Fig. 13a, it can be seen that the damping ratio of ballast specimen increases with the increase of rubber granules content, and the damping ratio of ballast specimen increases by 30.03%, 55.57%, and 63.55% for rubber granules content of 5%, 10%, and 15%. This is consistent with previous research [15]. This is due to the fact that the rubber granules are highly elastic substances, which can absorb part of the impact energy, and that the rubber granules are distributed between the ballast particles, expanding the stress distribution inside the specimen and increasing the movement of

the ballast particles. The degree of increase in the damping ratio of ballast specimens decreases when the rubber granule content exceeds 10%. Compared to the ballast specimens without geogrid, the ballast specimens with geogrid 100 mm away from the subgrade showed a decrease in damping ratio of 12.50%, 11.52%, 8.99%, and 3.42% at 0%, 5%, 10%, and 15% rubber granules content. The reduction in damping ratio of ballast specimens by geogrid decreases with the increase in rubber granule content. The geogrid restricts the movement, rotation and rearrangement of the ballast particles and reduces the dissipation of energy, thus leading to a decrease in the damping ratio of the specimen. Rubber granules increase the relative motion between ballast particles and weaken the interlock between the geogrid and ballast particles, resulting in a lesser reduction in the

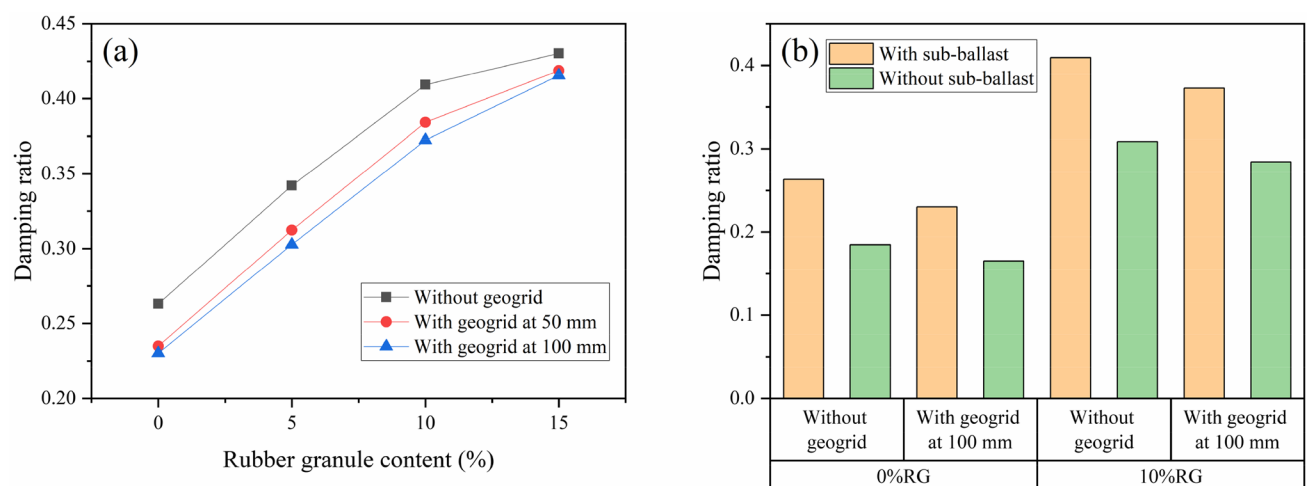


Fig. 13 Damping ratio of ballast with geogrid and rubber granules: **a** Damping ratio of ballast with sub-ballast; **b** Damping ratio of ballast with and without sub-ballast

Table 3 Stiffness and damping ratio of each group of ballast specimens

Test number	Subgrade type	Geogrid position	Rubber granule content (%)	Stiffness (N/m)	Damping ratio
T1	With sub-ballast	Without geogrid	0	1,602,217	0.2631
T2	With sub-ballast	Without geogrid	5	1,291,874	0.3421
T3	With sub-ballast	Without geogrid	10	1,000,122	0.4093
T4	With sub-ballast	Without geogrid	15	839,499	0.4303
T5	With sub-ballast	50 mm above the subgrade	0	1,830,692	0.2349
T6	With sub-ballast	50 mm above the subgrade	5	1,483,097	0.3124
T7	With sub-ballast	50 mm above the subgrade	10	1,087,430	0.3842
T8	With sub-ballast	50 mm above the subgrade	15	865,621	0.4187
T9	With sub-ballast	100 mm above the subgrade	0	1,892,303	0.2302
T10	With sub-ballast	100 mm above the subgrade	5	1,474,495	0.3027
T11	With sub-ballast	100 mm above the subgrade	10	1,110,116	0.3725
T12	With sub-ballast	100mm above the subgrade	15	885,026	0.4156
T13	Without sub-ballast	Without geogrid	0	2,370,755	0.1846
T14	Without sub-ballast	Without geogrid	10	1,262,842	0.3118
T15	Without sub-ballast	100 mm above the subgrade	0	2,542,650	0.1650
T16	Without sub-ballast	100 mm above the subgrade	10	1,341,890	0.2876

damping ratio. Figure 13b shows the damping ratios of ballast specimens with different subgrade stiffness. The damping ratio of the specimen without sub-ballast is smaller than that of the specimen with sub-ballast because the sub-ballast can absorb part of the impact energy. The addition of 10% rubber granules increased the damping ratio of the specimens with and without sub-ballast by 55.57% and 67.17%, which indicates that the rubber granules have a better effect on enhancing the damping ratio of the specimens on a rigid subgrade. The details of stiffness and damping ratio of ballast specimens are shown in Table 3.

4 Conclusions

In order to investigate the effect of the combination of geogrid and rubber granules on the performance of ballast under impact loads, this paper carried out a series of drop hammer impact tests on the ballast specimens with geogrid and rubber granules, investigated the effects of the geogrid laying position, rubber granules content and subgrade stiffness on the deformation, breakage, stiffness and damping ratio of the ballast specimens and analyzed the mechanism of its influence, and the main conclusions can be obtained are as follows:

1. The ability of rubber granules to reduce ballast deformation is limited (6.38% reduction in axial deformation and 2.31% reduction in radial deformation) because rubber granules absorb impact energy but reduce friction between ballast particles. The geogrid reduces the axial deformation of the specimen by 12.77% and the radial

deformation by 14.08% by restricting the movement of ballast particles. The combination of geogrid and rubber particles reduces the axial deformation of ballast specimen by 31.91% and radial deformation by 30.98%, which is better than that of geogrid or rubber granules alone.

2. With the increase of rubber granules content, the breakage of ballast specimens decreased by 11.63%, 31.42%, 52.48%, and the breakage of ballast was further reduced under the combined effect of geogrid and rubber granules.
3. Rubber granules can improve the damping ratio of ballast, but reduce the stiffness of ballast, affecting the stability of the track, while geogrid can improve the stiffness of ballast. The combination of geogrid and rubber granules enhances the damping ratio of ballast, reduces the degree of reduction of ballast stiffness, and maintains the stability of the track.
4. Ballast specimens without sub-ballast have greater deformation, breakage, and stiffness, and smaller damping ratio than ballast specimens with sub-ballast. Geogrid and rubber granules on rigid subgrade have better performance enhancement of ballast. As the sub-ballast absorbs impact energy and reduces vibration, it acts similarly to geogrids and rubber granules, leaving the advantages of both underutilized.

Considering the deformation, breakage, stiffness and damping ratio of ballast, geogrid at 100 mm above the subgrade and rubber granules with 10% by volume are the optimum combination of materials to enhance the performance of ballast. From the practical application, the

combination can reduce the deformation and degradation of ballast, maintain the stability of the track and extend the service life of the track.

Acknowledgements This work was financially supported by National Natural Science Foundation of China (NSFC) (Grant Nos. 51878521, 51178358). The support is gratefully acknowledged.

Author contributions The conception and design of the study, preparation of materials, data collection and analysis were performed by CL, RG and QH. The first draft of the manuscript was written by CL. The manuscript was revised and polished by CL, JC, RG and QH. All authors read and approved the final manuscript.

Data availability Some or all data or models, that support the findings of this study are available from the corresponding author upon reasonable request.

Declarations

Conflict of interest The authors all declare no conflict of interest.

References

- Bian, X.C., Li, W., Qian, Y., Tutumluer, E.: Analysing the effect of principal stress rotation on railway track settlement by discrete element method. *Geotechnique* **70**, 803–821 (2020)
- Indraratna, B., Ngo, T., Ferreira, F.B., Rujikiatkamjorn, C., Shahkolahi, A.: Laboratory examination of ballast deformation and degradation under impact loads with synthetic inclusions. *Transp. Geotech.* **25**, 17 (2020)
- Indraratna, B., Ngo, T., Rujikiatkamjorn, C.: Behavior of geogrid-reinforced ballast under various levels of fouling. *Geotext. Geomembr.* **29**, 313–322 (2011)
- Ngo, N.T., Indraratna, B., Rujikiatkamjorn, C.: Stabilization of track substructure with geo-inclusions- experimental evidence and DEM simulation. *Int. J. Rail Transp.* **5**, 63–86 (2017)
- Ngo, N.T., Indraratna, B., Ferreira, F.B., Rujikiatkamjorn, C.: Improved performance of geosynthetics enhanced ballast: laboratory and numerical studies. *Proc. Inst. Civ. Eng.-Ground Improv.* **171**, 202–222 (2018)
- Nimbalkar, S., Indraratna, B., Dash, S.K., Christie, D.: Improved performance of railway ballast under impact loads using shock mats. *J. Geotech. Geoenviron. Eng.* **138**, 281–294 (2012)
- Li, D.Q., Davis, D.: Transition of railroad bridge approaches. *J. Geotech. Geoenviron. Eng.* **131**, 1392–1398 (2005)
- Sweta, K., Hussaini, S.K.K.: Effect of shearing rate on the behavior of geogrid-reinforced railroad ballast under direct shear conditions. *Geotext. Geomembr.* **46**, 251–256 (2018)
- Esmaili, M., Pourrashnoo, A.: Experimental investigation of shear strength parameters of ballast encased with geogrid. *Constr. Build. Mater.* **335**, 12 (2022)
- Hussaini, S.K.K., Indraratna, B., Vinod, J.S.: Performance assessment of geogrid-reinforced railroad ballast during cyclic loading. *Transp. Geotech.* **2**, 99–107 (2015)
- Sweta, K., Hussaini, S.K.K.: Effect of geogrid on deformation response and resilient modulus of railroad ballast under cyclic loading. *Constr. Build. Mater.* **264**, 13 (2020)
- Indraratna, B., Hussaini, S.K.K., Vinod, J.S.: The lateral displacement response of geogrid-reinforced ballast under cyclic loading. *Geotext. Geomembr.* **39**, 20–29 (2013)
- Giroud, J.P., Han, J.: Design method for geogrid-reinforced unpaved roads. I. Development of design method. *J. Geotech. Geoenviron. Eng.* **130**, 775–786 (2004)
- Song, W.M., Huang, B.S., Shu, X., Wu, H., Gong, H.R., Han, B.Y., Zou, J.F.: Improving damping properties of railway ballast by addition of tire-derived aggregate. *Transp. Res. Rec.* **2673**, 299–307 (2019)
- Arachchige, C.M.K., Indraratna, B., Qi, Y.J., Vinod, J.S., Rujikiatkamjorn, C.: Deformation and degradation behaviour of Rubber Intermixed Ballast System under cyclic loading. *Eng. Geol.* **307**, 10 (2022)
- Koohmishi, M., Azarhoosh, A.: Stiffness and damping properties of railway ballast aggregate considering influence of degradation of aggregate and incorporation of crumb rubber. *Soil Dyn. Earthq. Eng.* **155**, 12 (2022)
- Fathali, M., Moghadas Nejad, F., Esmaili, M.: Influence of tire-derived aggregates on the properties of railway ballast material. *J. Mater. Civ. Eng.* **29**, 9 (2017)
- Sol-Sánchez, M., Thom, N.H., Moreno-Navarro, F., Rubio-Gámez, M.C., Airey, G.D.: A study into the use of crumb rubber in railway ballast. *Constr. Build. Mater.* **75**, 19–24 (2015)
- Sol-Sánchez, M., Moreno-Navarro, F., Martínez-Montes, G., Rubio-Gámez, M.C.: An alternative sustainable railway maintenance technique based on the use of rubber particles. *J. Clean. Prod.* **142**, 3850–3858 (2017)
- Koohmishi, M., Azarhoosh, A.: Degradation of crumb rubber modified railway ballast under impact loading considering aggregate gradation and rubber size. *Can. Geotech. J.* **58**, 398–410 (2021)
- Gong, H.R., Song, W.M., Huang, B.S., Shu, X., Han, B.Y., Wu, H., Zou, J.F.: Direct shear properties of railway ballast mixed with tire derived aggregates: experimental and numerical investigations. *Constr. Build. Mater.* **200**, 465–473 (2019)
- Arachchige, C.M.K., Indraratna, B., Qi, Y.J., Vinod, J.S., Rujikiatkamjorn, C.: Geotechnical characteristics of a Rubber Intermixed Ballast System. *Acta Geotech.* **17**, 1847–1858 (2022)
- Zhang, F.G., Chang, J.M., Feng, H.P.: Laboratory study on degradation of ballast mixed with crumb rubber under impact loads. *Int. J. Rail Transp.* **23**, 767–789 (2022)
- Nimbalkar, S., Indraratna, B.: Improved performance of ballasted rail track using geosynthetics and rubber shockmat. *J. Geotech. Geoenviron. Eng.* **142**, 13 (2016)
- Nimbalkar, S., Neville, T., Indraratna, B.: Performance assessment of reinforced ballasted rail track. In: *Ground Improvement: Proceedings of the Institution of Civil Engineers.* (2014)
- Khoshoei, S.M., Bak, H.M., Abtahi, S.M., Hejazi, S.M., Shahbodagh, B.: Experimental investigation of the cyclic behavior of steel-slag ballast mixed with tire-derived aggregate. *J. Mater. Civ. Eng.* **33**, 11 (2021)
- Sol-Sánchez, M., Moreno-Navarro, F., Pérez, R., Rubio-Gámez, M.C.: Defining the process of including sustainable rubber particles under sleepers to improve track behaviour and performance. *J. Clean. Prod.* **227**, 178–188 (2019)
- Chen, C., McDowell, G.R., Thom, N.H.: Discrete element modelling of cyclic loads of geogrid-reinforced ballast under confined and unconfined conditions. *Geotext. Geomembr.* **35**, 76–86 (2012)
- McDowell, G.R., Harireche, O., Konietzky, H., Brown, S.F., Thom, N.H.: Discrete element modelling of geogrid-reinforced aggregates. *Proc. Inst. Civ. Eng. Geotech. Eng.* **159**, 35–48 (2006)
- Brown, S.F., Kwan, J., Thoma, N.H.: Identifying the key parameters that influence geogrid reinforcement of railway ballast. *Geotext. Geomembr.* **25**, 326–335 (2007)
- McDowell, G., Stickley, P.: Performance of geogrid-reinforced ballast. *Ground Eng.* **39**, 26–30 (2006)

32. Indraratna, B., Nimbalkar, S., Christie, D., Rujikiatkamjorn, C., Vinod, J.: Field assessment of the performance of a ballasted rail track with and without geosynthetics. *J. Geotech. Geoenviron. Eng.* **136**, 907–917 (2010)
33. Zhai, W.M., Wang, K.Y., Lin, J.H.: Modelling and experiment of railway ballast vibrations. *J. Sound Vib.* **270**, 673–683 (2004)
34. Argatov, I.I.: Mathematical modeling of linear viscoelastic impact: application to drop impact testing of articular cartilage. *Tribol. Int.* **63**, 213–225 (2013)
35. Choi, J.: Influence of track support stiffness of railway tracks on track impact factor. *J. Eng. Mech.* **140**, 12 (2014)
36. Choi, J.Y., Kim, S.H.: Qualitative prediction model for dynamic behavior of ballasted tracks. *Appl. Sci.-Basel* **10**, 18 (2020)
37. Indraratna, B., Lackenby, J., Christie, D.: Effect of confining pressure on the degradation of ballast under cyclic loading. *Géotechnique* **55**, 325–328 (2005)

Publisher's Note Springer Nature remains neutral with regard to jurisdictional claims in published maps and institutional affiliations.

Springer Nature or its licensor (e.g. a society or other partner) holds exclusive rights to this article under a publishing agreement with the author(s) or other rightsholder(s); author self-archiving of the accepted manuscript version of this article is solely governed by the terms of such publishing agreement and applicable law.